International Research Journal of Engineering and Technology (IRJET) e-ISSN: 2395-0056
Volume: 07 Issue: 12 | Dec 2020 www.irjet.net p-ISSN: 2395-0072

A Computational Study on Improving Magnus force

Jay Baviskar[1]

[1]*Department of Mechanical Engineering, University of Mumbai, India*

Abstract - *Magnus effect is a phenomenon popularly known for its influence on the curved flight paths of spinning balls. Besides on ball games, most extensive studies & research are carried out on rotating cylinders for its potentiality in replacing airfoils & other applications. In this paper, various numerical simulations are conducted and analysed in ANSYS with Fluent. Different parameters like Reynolds number, aspect ratio, RPM of the cylinder, its roughness & their effects are studied. The study aims to find the most optimal parameters for its operation in any area of application as well as tests a method to improve the aerodynamic efficiency (drag & lift coefficients) even more.*

Key Words: CFD study, Magnus effect, Laminar-Turbulent Boundary layer transition, Critical Reynolds no., Rotating cylinders

1.INTRODUCTION

1.1 Magnus effect

The Magnus effect is a phenomenon in which spinning objects experience a force perpendicular to the direction or line of motion.

The phenomenon was first studied by Sir Isaac Newton who wrote a paper on this subject in 1607. Until then, the curvilinear flight paths were just considered an optical illusion. The subject was then again revived by Gustav Magnus, a German physicist, who conducted an experiment and became the first man to demonstrate that spinning objects experience a sideways force when moved through fluids. The history & experiment setup is quite well elaborated by J. Seifert in his paper [1].

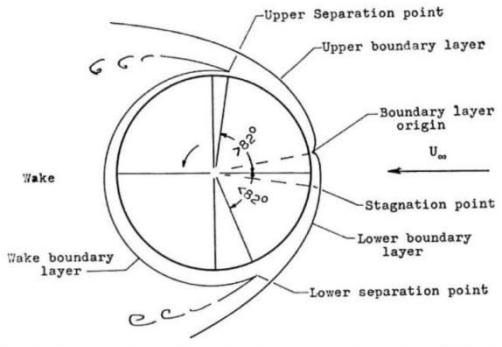

Figure 1 – Schematic representation of asymmetric boundary layers around a rotating sphere/cylinder

1.2 Explanation

A simplified explanation for Magnus effect is given by Bernoulli's potential theory. With reference to it, an increase in the fluid velocity occurs with a decrease in pressure of fluid. Thus, in case of a spinning rotating cylinder or a sphere rotating in anti-clockwise direction, the lower part of it interferes with the fluid flow thereby reducing the velocity. A relative increase in velocity is associated with a relative decrease in pressure and thus, the unequal pressure differences above & below, the ball deviates from its path.

Bernoulli's theory holds true for inviscid flows and for smooth surfaces lest not. A more accurate explanation of this is given by Prandtl's boundary layer theory. It also explains the special case of inverse Magnus effect occurring only for a brief period when both – the upper and lower surfaces of the object undergo complete boundary layer transition from laminar to turbulent.

Later in 1961, Swanson explained that the Magnus force induced is the resultant of asymmetric formation of boundary layers above and below the spinning objects. In case of same example fig. 1, The angular distance of transition point and flow separation from the frontal nose or boundary layer origin (stagnation point) is more on the upper side(>82°) than the lower side(<82°). Consequently, the earlier separation and wake formation on the lower side results in the cylinder experiencing an upward force.

1.3 Examples

The examples of Magnus effect can easily and quite clearly be seen in many ball sports like football, tennis, table tennis, baseball & cricket, wherein players clearly seem to take advantage of it.

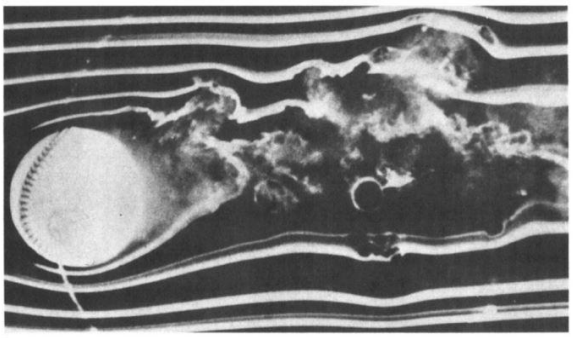

Figure 2 – Smoke photograph of a spinning baseball. By F. N. M Brown, Notre Dame University (Brown 1971)

Another glimpse of this phenomenon could be seen in external ballistics. Benjamin Robbins studied that a bullet acquires a whirling motion he concluded in his 1805 paper that the air resistance "will be increased in that part where the whirling motion conspires with the progressive one" [1]. Similar effects have to be considered & taken care of while launching missiles. Applicative areas are hard to come by but several attempts have been successful in harnessing this force. The best examples of this would be the Flettner rotor ship and an airplane using rotating cylinders instead of a conventional wing to generate lift.

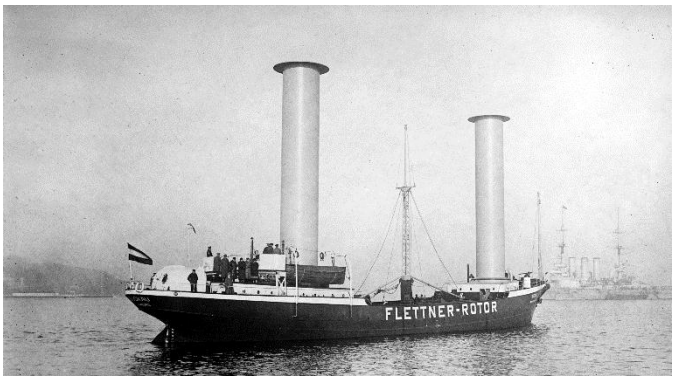

Figure 3 – Flettner rotor ship. Courtesy of The Library of Congress

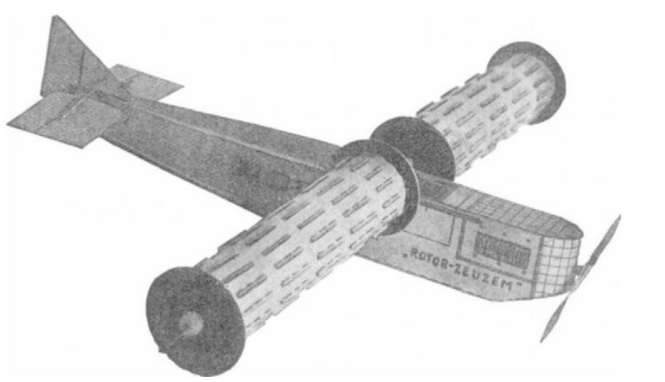

Figure 4 – Model of Rotor-Zeuzem. Courtesy of Deutsches Museum Archiv.

2. GEOMETRY

All the numerical simulations are conducted on a cylinder of diameter 0.1m & length 0.5m. The size of the flow domain is 2m x 1.2m x 1.1m. The dimensions were decided on the possibility of conducting further experimental studies in the wind tunnel to validate these numerical results.

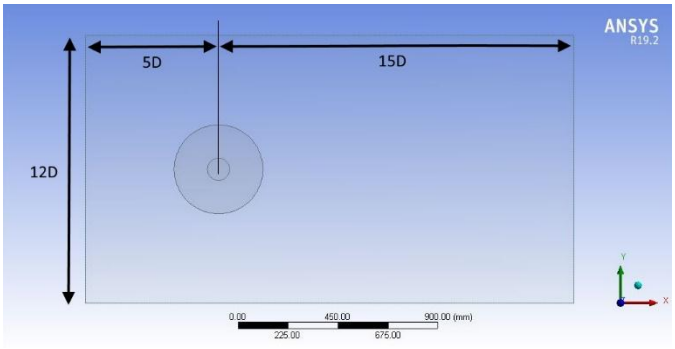

Figure 5 – Geometry of the model.

The domain extends 15D downstream & 5D upstream of the cylinder, which is sufficient for developing full flow conditions. The cross-sectional area of flow domain is 1.32m^2, resulting in a blockage ratio of 3.7% which is less than recommended of 5%.

$$\text{Blockage ratio} = \frac{\text{Projected frontal area of test object}}{\text{Frontal area of flow domain}}$$

$$= \frac{0.05}{1.32} = 0.037$$

3. MESH

2 methods were adopted for meshing the geometry -

1. Unstructured tetrahedral mesh
2. Structured mesh using Cutcell

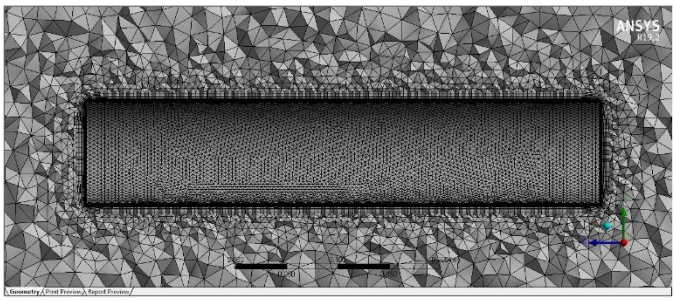

Figure 6 – Tetrahedral mesh near cylinder.

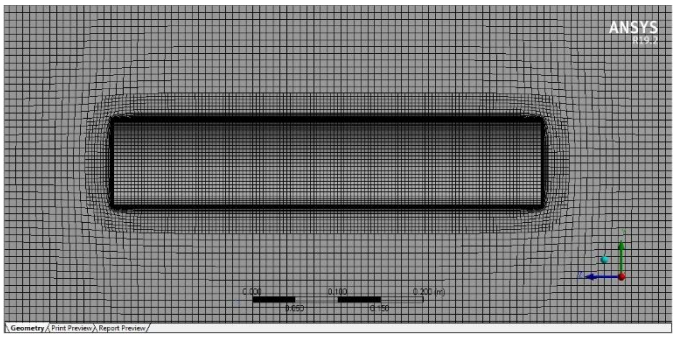

Figure 7 – Structured mesh by Cutcell method in cylinder region.

Multiple trials were conducted on both the mesh. The unstructured tetrahedral mesh provided a little more accurate and stable results than Cutcell. Thus, tetrahedral mesh was finalised to conduct further studies. The flow domain consisted of approx. 1 million cells.

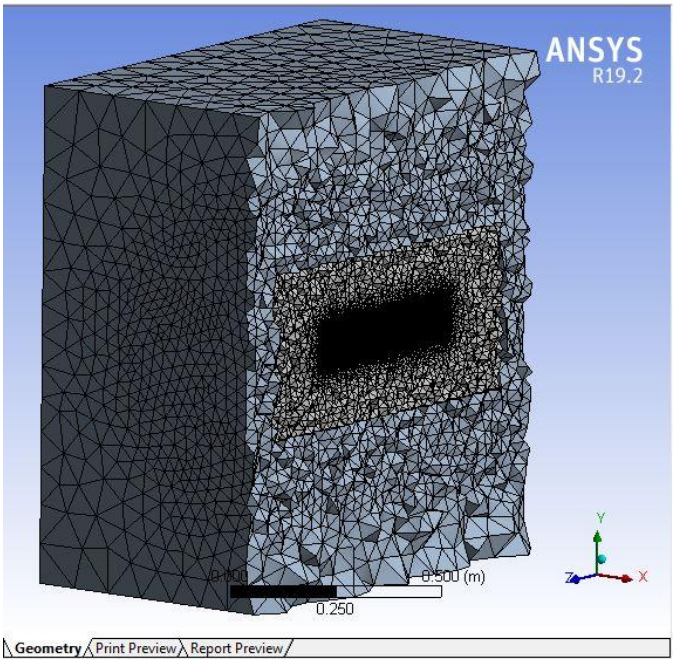

Figure 8 – Sectional view of mesh of the flow domain.

Face sizing of 4mm was applied on the cylinder to make the mesh finer near the cylinder. Cell sizing of 10 mm was also implemented on the contact region to ensure a smoother growth rate of cells.

Inflation layers were also adopted on the surface of the cylinder to resolve the boundary layers (Refer fig. 6). Fluent recommends a mesh which keeps the y+ values between 1 to 5 adjoining the wall boundary. The thickness of the first layer of the grid cells was calculated by keeping y+ value as 1 at 25k Re.
Following equations & methodology is adopted from ANSYS Fluent v15 leaflet [8]

$C_f = 0.058Re^{-0.2}$
$= 0.058 \times 25{,}000^{-0.2}$
$= 7.653 \times 10^{-4}$

$\tau_w = C_f \rho U_\infty^2$
$= 7.653 \times 10^{-4} \times 1.225 \times 3.66^2$
$= 6.279 \times 10^{-3}$

$U\tau = \sqrt{\frac{\tau w}{\rho}} = \sqrt{\frac{0.00627}{1.225}} = 0.071$

$y = \frac{(y+)\,\mu}{U\tau\,\rho} = (1 \times 1.7894 \times 10^{-5})/(0.071 \times 1.225)$

$= 2.05 \times 10^{-4}$

Where,

C_f = skin friction, Re=Reynolds number, τ_w=wall shear stress, Uτ=friction velocity, ρ=density of fluid (1.225 kg/m^3, μ=dynamic viscosity of air (1.7894×10^{-5})

This means that the first layer of grid should be approx. 0.2 mm. It also corresponds to y+ value of 100 at Re 1 million, but it is acceptable since y+ values up to 500 are acceptable for high Reynolds number [6].

3. BOUNDARY CONDITIONS

A Multiple Reference Frame method (MRF) was used for the simulation since the experiment consisted of a spinning cylinder. Also, the inner cylindrical enclosure provided more flexibility for making a finer mesh in the cylinder region.
The study was conducted on a total of 5 Reynold numbers. 2 of them could be found in the laminar pre-critical region, 2 in the transition & 1 in the post-critical region. Table 1 illustrates the chosen Reynolds numbers and their corresponding inlet velocity for ρ=1.225, l=0.1, $\mu=1.7894 \times 10^{-5}$

Reynolds number	Inlet velocity
25,000	3.66 m/s
100,000	14.6 m/s
250,000	36.5 m/s
750,000	109.5 m/s
1,000,000	146 m/s

Table 1 – Reynolds number & their corresponding inlet velocity

Velocity ratio is defined as the circumferential velocity of the cylinder to the free stream velocity. For example, at 25,000 Reynolds number and velocity ratio to be 1, the circumferential velocity of the cylinder should be the same as fluid velocity. The relation between angular and linear velocity is given by

$V = r \times w$

Hence for cylinder dia. 0.1m & velocity 3.66 m/s, we have

$w = v/r = 3.66/0.05 = 73.2$ rps

A total of 5 velocity ratios were chosen. The following table lists out the angular velocity of the cylinder in order to obtain the desired velocity ratios for the 1st case.

Velocity ratio, r	Angular velocity of cylinder, RPS
0.5	36.6 rps
1	73.2 rps
1.5	109.8 rps
2	146.4 rps
3	219.6 rps

Table 2 – Rotation speeds at different velocity ratios

Similarly, all other rotation speeds were calculated for all the other test cases and given as a moving wall boundary condition.

For the calculation of lift & drag coefficients,

Characteristic length = diameter of cylinder = 0.1 m
Reference area = frontal projected area of cylinder = 0.5 x 0.1 = 0.05 m^2

4. COEFFICIENT OF DRAG FOR A STATIC CYLINDER

Innumerable numerical and experimental studies have been conducted on flow past cylinders at various Reynolds numbers. The coefficient of drag of a 2D smooth circular cylinder i.e infinitely long cylinder lies between 1.15-1.2 within sub-critical region [4]. However, in case of real 3D bodies of finite length, Cd is largely dependent on the length or aspect ratios and other boundary conditions.

In case of cylinders, Cd decreases with decreasing length(L) of cylinders and is defined in terms of a dimensionless aspect ratio (L/D). The design guidance by DNVGL[X] on calculating Cd with respect to the aspect ratio of cylinder is presented in the following table

L/D	2	5	10	20	40	50
k	0.58	0.62	0.68	0.74	0.82	0.87

Table 3 – Drag reduction factors for cylinders with different aspect ratios [2]

K - called as the Drag reduction factor is defined by

$$K = \frac{Cd\ finite}{Cd\ \infty}$$

The origins of these drag reduction factors have not been cited by DNVGL but it is presented in the earliest version of design guidance [3]. In our case, the cylinder has an aspect ratio of 5, thus
Cd = 0.62 * 1.2 = 0.74

A test trial was run with free stream velocity of 3.66m/s i.e at Reynolds number of 25,000. Simple Laminar model was utilised to simulate the flow. The coefficient of drag was found to be 0.72 which closely met the expected value of 0.74.

Another experimental study by Goittengen was conducted on cylinders with finite lengths. The following table represents the results [5]

L/d	Cd
1	0.62
1.98	0.67
2.96	0.73
5	0.72
10	0.8

Table 4 – Results of Goittengen on various L/d

The solution closely matches with both the sources and so further simulations could be run.

5. EFFECT OF REYNOLDS NUMBER ON ROTATING CYLINDER

In all the test cases, the density, dynamic viscosity, temperature of the air & diameter of the cylinder are constant. Therefore, the only thing which would change the Reynolds number is the free stream velocity of the fluid.

To have a better understanding, velocities corresponding to the same Reynolds number from Table 1 have been used. The rotation is kept constant at 73.2 RPS.

In fig. 9, we can clearly see that as Reynolds number increases, the drag reduces gradually at a slow rate. On the other hand, lift coefficient increases and drops down suddenly after a point. The point at which max lift coefficient has been observed corresponds to Re 25k and the velocity ratio of 1.

From this we can conclude that lift generation is not in effect over a wide range of Reynolds number.

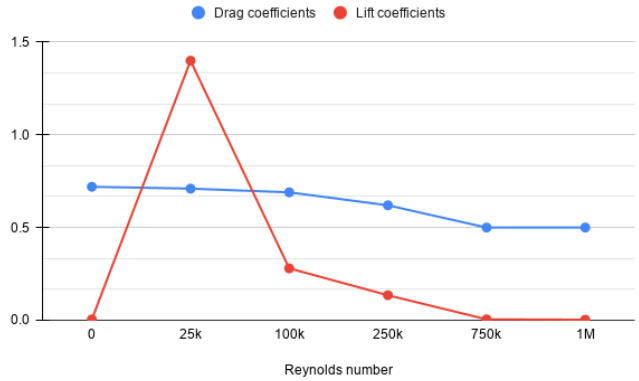

Figure 9 – Reynolds number vs Force coefficients

6. EFFECT OF VELOCITY RATIO ON ROTATING CYLINDER

The aerodynamic characteristics of Magnus force are greatly dependent on velocity ratio of circumferential velocity to free stream velocity of fluid.

5 simulations are conducted on 5 different velocity ratios – 0.5, 1, 1.5, 2 & 3 on the same Reynolds number i.e for the first case, 25k.

The flow was considered purely laminar & so laminar model was utilized.

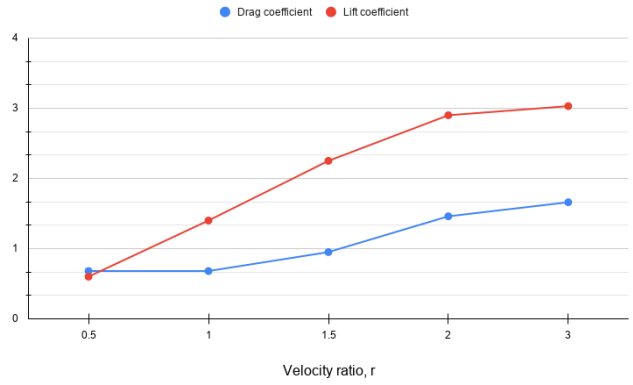

Figure 10 – Force coefficients vs Velocity ratio at 100k Re

The graphs clearly show that with increasing velocity ratio, both the force coefficients increase.

Vortex shedding or popularly known as Karman vortices is a phenomenon associated with laminar flow over cylinders forming eddies alternately on each side. Some simulations clearly depicted that the shedding occurred along with the Magnus effect.

In case of spinning cylinders, shedding occurs at low Re's & ceases or achieves a quasi-steady-state as the velocity ratio increases. Fig. 11 shows consistent fluctuations in the graph of Cl exhibiting the shedding. In such cases the average Cl was taken into accounts for further comparisons.

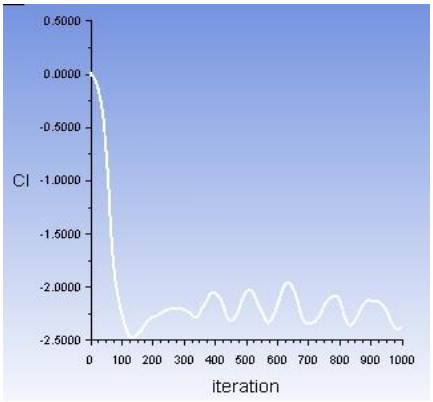

Figure 11 – Lift coefficient plot at r=1.5 & Re=100k

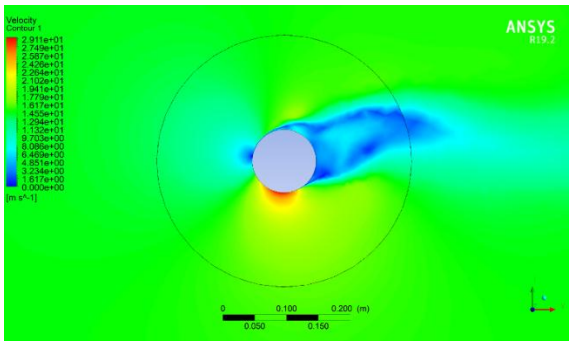

Figure 12 – Velocity contours at r=1.5 & Re=100k exhibiting Magnus effect as well as vortex shedding.

Similar simulations were conducted on rest of the Reynolds numbers in combination with 5 velocity ratios. The later test cases from 250k Re onwards were run using K-w SST model. K-w models perform far superior than k-e for complex boundary flows under adverse pressure gradients. K-w SST turbulence model also predicts flow separation more accurately than any other RANS model [8].

1st order schemes were implemented to obtain stable soln. In most cases, the residuals were converged up to 10^{-5}

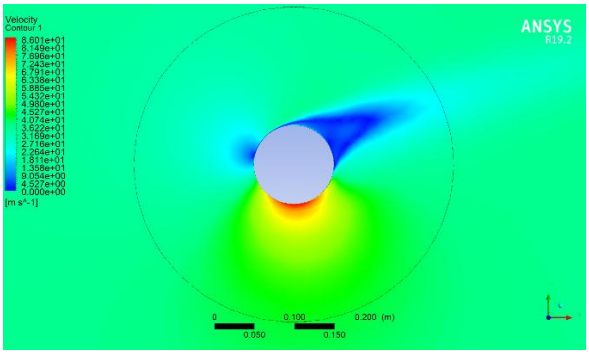

Figure 13 – Velocity contours at 250k Re & velocity ratio 1.5

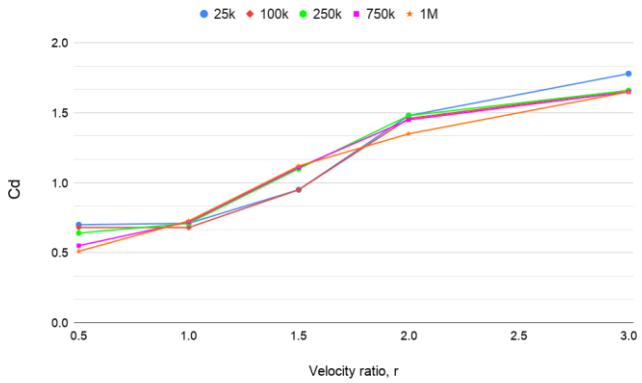

Figure 14 – Velocity ratio vs Cd at different Reynolds number

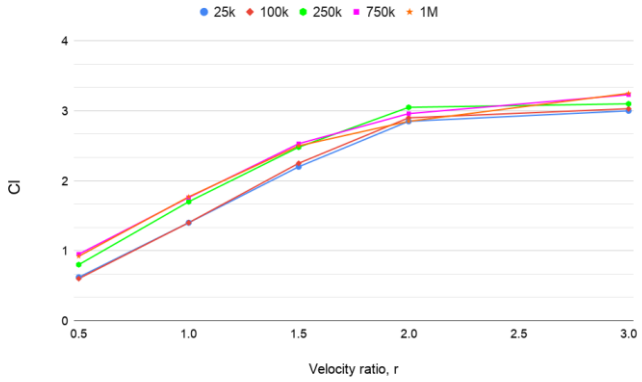

Figure 15 – Velocity ratio vs Cl at different Reynolds number

Fig. 15 clearly show that with increasing velocity ratio, lift coefficient increases. It is also evident that drag coefficient increases along with it. More the velocity ratio, more the lift coefficient, which is just a perfect alternative for airfoils but the problem lies with drag. At higher velocity ratios, the skin friction takes up a bigger role in overall drag and reduces the Cl/Cd ratio.

The main motive of the study was the Cl/Cd ratio. The expected outcome was maximum Cl/Cd ratio in the super-critical region where the boundary layer transforms completely into a turbulent one, at around Re 750k. Instead, there was no such pattern to be found. However, from graph and fig. 16, at each Reynolds number, maximum Cl/Cd was found to be at a velocity ratio r=1 or 1.5.

Another surprising finding was that after 250k Re, the force coefficients were found almost to be same at same velocity ratios. Perhaps, more tests in early pre-critical range should lead to new findings.

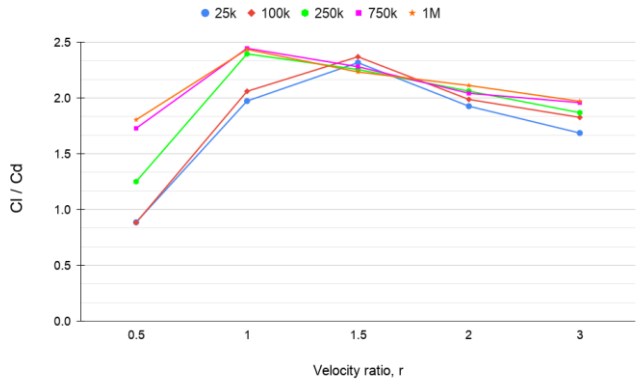

Figure 16 – Cl/Cd vs velocity ratio at different Reynolds nos.

7. EFFECT OF DISCS ON ROTATING CYLINDERS

Many studies and trials have been conducted to increase the lift coefficient of rotating cylinders by means of small changes in design parameter. One such method is by attaching discs at the end of the cylinders.

The open ends of the cylinder causes it to generate tip vortices thereby reducing the effective aspect ratio thereby ultimately leading to the loss of lift generation.

A simulation was run on one of the above cases at Re 250k & r=1.5. It was evident from the pressure contours that the effective aspect ratio on the cylinder was increased (blue low-pressure zone). The lift coefficient increased from 2.45 to a staggering 3.4!

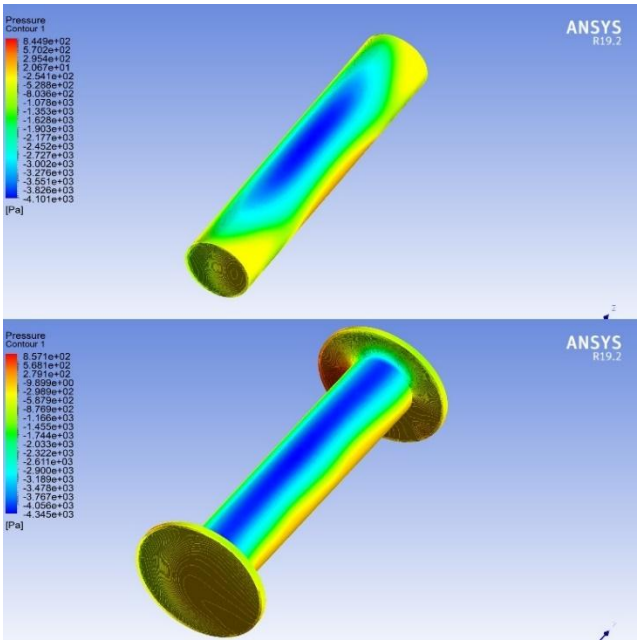

Figure 17 – the increment in effective aspect ratio after attaching disc

More detailed study on sizes of discs & their effect on Magnus force has been done by Thom A in his paper [9].

8. EFFECT OF ROUGHNESS ON ROTATING CYLINDERS

The nature of flow around rough cylinders is found to be the same as in cases of spheres. The coefficient of drag remains constant during the pre-critical region & starts dropping after crossing Reynolds number of approximately 200k-250k.

Increasing the surface roughness on the cylinder promotes premature transition of boundary layers - from laminar to turbulent. The introduction of surface roughness delays the separation of the turbulent boundary layer resulting in formation of smaller wakes. However, it increases the skin friction drag over the whole body. Since form drag has a bigger contribution in drag force, there is a drop in Cd and the drop starts at an earlier stage, at a lower Reynolds number.

However, very few studies have been undertaken on the effect of surface roughness on spinning cylinders and nature of flow. A study by Thom A. in the mid-1950s examined the effects by gluing sand roughness on the cylinders (no sizing or relative sizing specified) for 33k<Re<93k. The results were rather disappointing and the lift & drag coefficients were only slightly more than the smooth one [10].

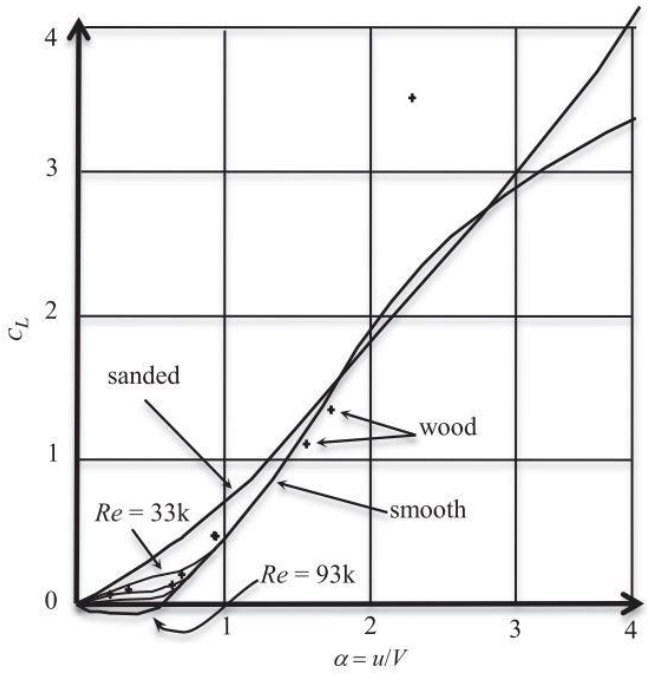

Figure 18 – Effect of surface roughness on Cl. Data by Thom, Recreated by Seifert J.

The main objective of studying the effect of surface roughness on rotating cylinders is to check whether the laminar-turbulent boundary layer transition can be triggered at lower Reynolds numbers & the possibility of better Cl/Cd ratio. A study by Lou et al. suggests that such triggering is possible, but only at certain roll angles [1]

9. CONCLUSIONS

1. From study above, we can certainly conclude that a significant increase in Magnus force is associated with an increase in velocity ratio and not of Reynolds number.
2. With a decrease in aspect ratio of cylinders, a decrease in drag coefficient is associated.
3. Keeping all the boundary conditions and design parameters the same, the lift coefficient of rotating cylinders of finite length can be significantly increased just by increasing the effective aspect ratio i.e., attaching discs at the end.
4. Pertaining to this study, max Cl/Cd were found to be in velocity ratio range of r=1-1.5. However, more no. of test cases must be studied in the pre-critical range to make this sure. Once this is confirmed, optimal parameters like angular velocity, aspect ratio & Reynolds no. could be reverse engineered for its efficient operation in applications.

REFERENCES

[1] J. Seifert, "A review of the Magnus effect in aeronautics," Prog. Aerospace. Sci. 55, 17–45 (2012).

[2] DNV GL, 'Environmental Conditions and Environmental Loads', Recommended Practice DNVGL-RP-C205. Det Norkse Veritas Germanischer Lloyd, 2017.

[3] DNV, 'Environmental Conditions and Environmental Loads', Classification Note CN-30.5. Det Norkse Veritas, 1991.

[4] Hoerner, Sighard F., Fluid-Dynamic Drag: Practical Information on Aerodynamic Drag and Hydrodynamic Resistance, 2nd ed. Dr. Sighard F. Hoerner, 1965.

[5] Fariver, D. J., 'Turbulent Uniform Flow around Cylinders of Finite Length', AIAA Journal, Vol. 19, No. 3, Mar-1981, pp. 275–281, DOI: 10.2514/3.7771.

[6] John Middendorf, "CFD Modeling of Wind Tunnel Flow Over Rotating Cylinder", Computational Fluid Dynamics, Professors Tracie Barber/Eddie Leonardi, May 30, 2003.

[7] W. M. Swanson, "The Magnus Effect: A Summary of Investigations to Date", Journal of Basic Engineering, Vol.83, 1961, pp. 461–470.

[8] ANSYS Fluent v15 Turbulence leaflet

[9] Thom A. Effect of discs on the air forces on a rotating cylinder. Aeronautical Research Committee, Reports and Memoranda 1934;1623.

[10] Thom A, Sengupta SR. Air torque on a cylinder rotating in an air stream. Aeronautical Research Committee, Reports and Memoranda 1932;1520.